Electronic Supplementary Material (ESI) for Nanoscale.

Supplementary Information

Tuning oxygen evolution reaction on nickel-iron alloy via active straining

Anqi Wang,[‡a] Zhonglong Zhao,[‡b] Di Hu,[a] Junfeng Niu,[c] Man Zhang,[a] Kai Yan,[*a] and Gang Lu[*b]

[a] Guangdong Provincial Key Laboratory of Environmental Pollution and Remediation Technology, School of Environmental Science and Engineering, Sun Yat-sen University, 135 Xingang Xi Road, Guangzhou, 510275, China
[b] Department of Physics and Astronomy, California State University Northridge, Northridge, CA 91330, USA
[c] Research Center for Eco-Environmental Engineering, Dongguan University of Technology, Dongguan 523808, China
‡ These Authors contributed equally to this work.
[*]Corresponding author: Kai Yan (E-mail: yank9@mail.sysu.edu.cn); Gang Lu (E-mail: ganglu@csun.edu)

Supporting Information Contains:

Experimental details

Materials

Nickel (Ni) Evaporation Pellets (1/4" Dia. x 1/2" Length, 99.995% purity) and Iron (Fe) Evaporation Pellets (1/4" Dia. x 1/2" Length, 99.995% purity) were purchased from Lesker. Acetone (ACS reagent, 99.5%) was purchased from Sigma-Aldrich and sodium hydroxide (NaOH, 96.7%) was purchased from Macron Chemicals.

Thin-film deposition

Thin metal films of Ni_3Fe were deposited by DC-magnetron sputtering on PMMA substrates (base vacuum 10^{-6} Torr), at deposition rates of 0.9 Å/s to 1.2 Å/s. Before the deposition of Ni_3Fe, ~6 nm Ti was firstly deposited to enhance the adhesion. The thickness of all films in this study was 20 nm, which is controlled by a thickness monitor.

Characterization of the deposited thin films

X-ray diffraction (Rigaku D-Max2200 VPC) using monochromatic Cu Kα radiation (40 kV, 40 mA, the scanning rage of 2 theta was from 9° to 90° at 10° min^{-1}) was carried out on the deposited thin films (Fig. S1), which revealed that the films had predominantly (111) orientation. X-ray photoelectron spectroscopy (XPS) studies were operated on an EscaLab 250 X-ray photoelectron spectrometer (Thermo Scientific, USA) with a pass energy of 20 eV and a monochromatized Al Kα as the excitation source at 150 W, the energy step size is 0.05 eV $step^{-1}$. Scanning electron microscopy (SEM) images were recorded using a Gemini500 instrument (Zeiss/Bruker, GER) at the accelerating voltage of 20 kV. The inductively coupled plasma optical emission spectrometer energy (ICP-OES) was performed on 5300DV (Perkin Elmer, USA) Transmission electron microscopy (TEM) patterns were taken on a FEI Tecnai G^2 F20 transmission electron microscope operated at 200 kV accelerating voltage. Atomic force microscope (AFM) was performed on a MFB-3D instrument (Asylum Research, UK) in tapping mode.

Electrochemical measurements

Electrochemical studies were carried out in a standard three electrode system controlled by a Metro (Multi Autolab 204) electrochemistry workstation. In all experiments, an Ag/AgCl reference electrode was employed and Pt coiled wire was used as counter electrode. 0.1 M NaOH solution was used as the electrolyte, which was prepared by dissolving the calculated amount of NaOH with the conductivity of 0.056 s/m water (at 25 °C) to form 0.1 M solution. The electrolyte was sparged with ultra-high purity argon (99.999%); all potentials reported in this paper are converted to the pH-independent reversible hydrogen electrode (RHE) scale. All experiments were repeated three times to confirm reproducibility. The electrochemical measurements were conducted in a three-electrode cell which was fabricated to be integrated with an Instron Model 5982 universal mechanical testing machine; the experimental setup is illustrated in Fig. 1. The design and the connection of the as-obtained metal film as working electrode are shown in Fig. S3. This setup allows *in-situ* measurements of electrochemical responses while the specimen is under uniaxial tension and compression. The scan rate of all electrochemical measurements was 50 mV/sec.

Voltage change measurements

In order to measure the potential shift due to strain, the difference between the reduction portion of the CVs corresponding to the strained and unstrained cases was obtained in a suitable current density range. The current density range was chosen such that the response was purely Faradaic in nature (corresponding to O_2 evolution electrocatalysis) as opposed to capacitive current. The error bars shown in Fig. 1d include the spread in the variation within the current range described above, as well as the sample-to-sample variation.

Computational methodology

The free energy of the OER intermediates, *OH, *O, and *OOH, are calculated relative to H_2O and H_2, as in the equations: $\Delta G_{*OH} = G_{*OH} + 1/2G(H_2) - G_{*} - G(H_2O)$, $\Delta G_{*O} = G_{*O} + G(H_2) - G_{*} - G(H_2O)$, and $\Delta G_{*OOH} = G_{*OOH} + 3/2G(H_2) - G_{*} - G(H_2O)$, where G_{*OH}, G_{*O}, G_{*OOH}, $G(H_2)$, and $G(H_2O)$ are the electronic ground state energies of *OH, *O, *OOH, gas phase H_2, and liquid H_2O plus the zero-point energy, -TS, and solvent corrections that taken from previous work.[1] A four-layer slab was used to simulate the Ni_3Fe (111) surface. The atoms in the bottom two layers were fixed while in the remain layers were fully relaxed. To avoid interactions between periodic images, a vacuum layer of 15Å is added to the adjacent slabs. Spin-polarized DFT calculations were carried out using the Vienna *ab initio* simulation package (VASP).[2] The Perdew-Burke-Ernzerhof functional within the generalized gradient approximation[3] and the projector augmented wave pseudopotential[4] were used in the calculations. An energy cutoff of 400 eV was used for the plane-wave basis set. The Brillouin zone was sampled on the basis of the Monkhorst-Pack scheme[5] with a 3×3×1 k-point mesh. The force convergence criterion for atomic relaxation was 0.02 eV/Å.

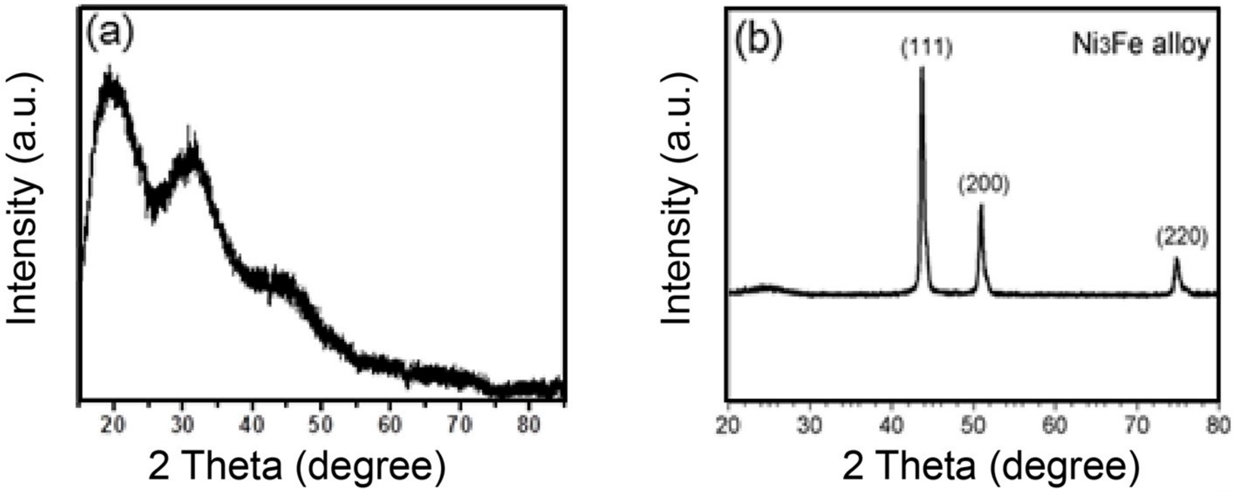

Fig. S1. The diffraction pattern of PMMA substrate (a) and the as-obtained 20 nm Ni_3Fe films on silicon substrate (b).The XRD pattern mainly present the peaks of PMMA substrate, while the predominantly (111) orientation was present on the silicon on the same batch.

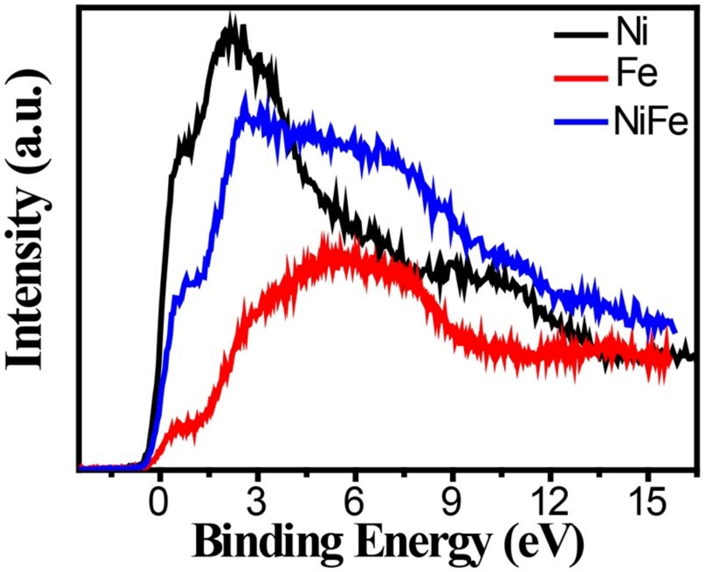

Fig. S2. Valence band of the Ni_3Fe compared to Ni and Fe film.

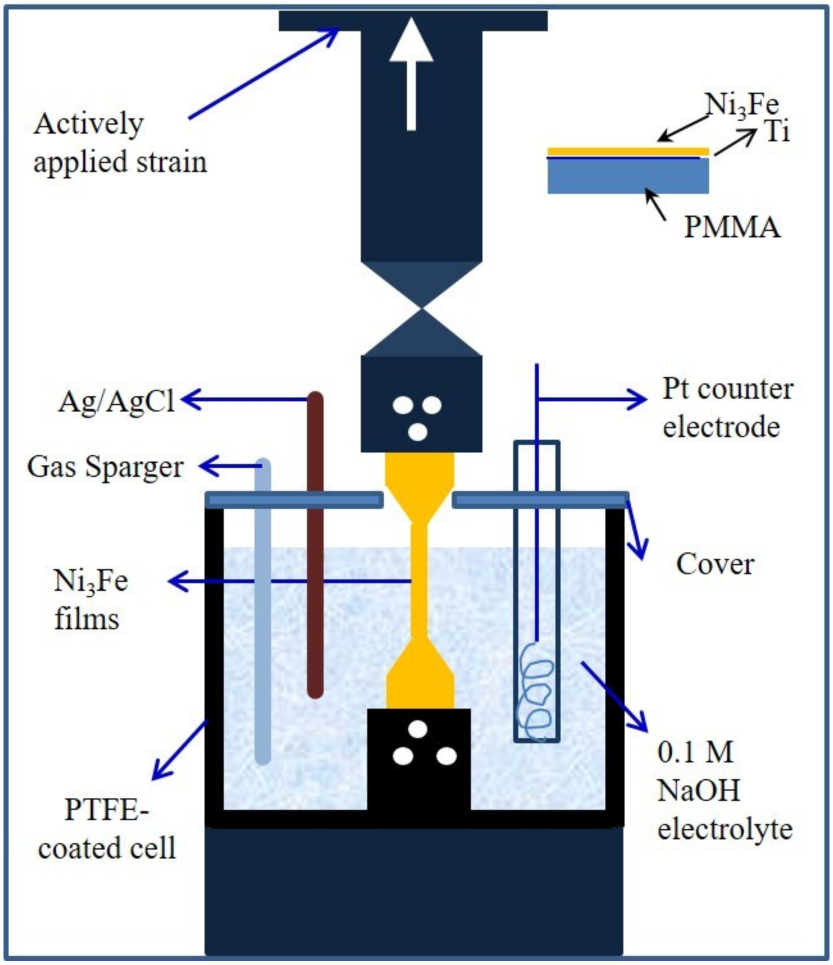

Fig. S3. Experimental setup to subject thin Ni_3Fe films to active strain by applying compressive or tensile loading. This setup is similar to our previous work.[6]

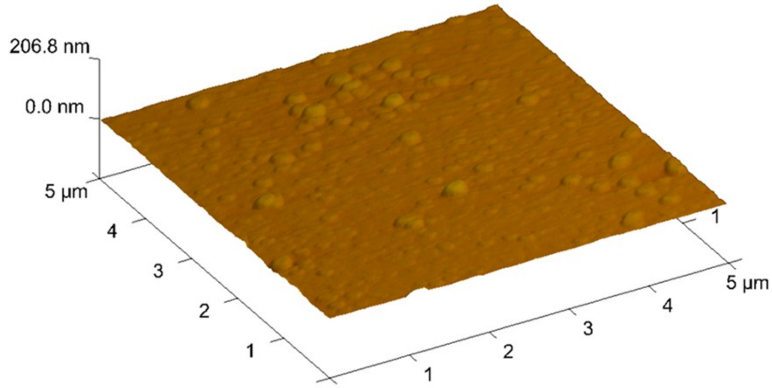

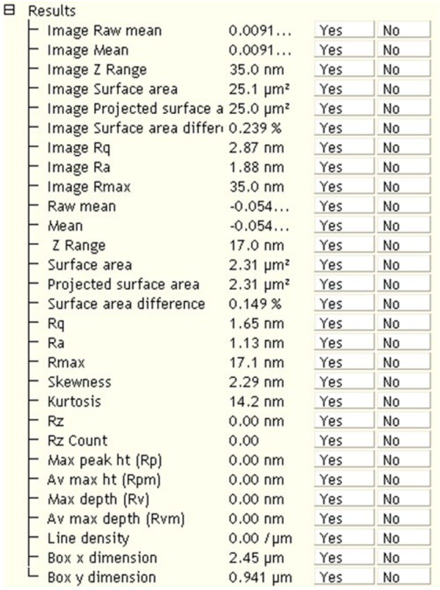
Results

Image Raw mean	0.0091...	Yes	No
Image Mean	0.0091...	Yes	No
Image Z Range	35.0 nm	Yes	No
Image Surface area	25.1 µm²	Yes	No
Image Projected surface a	25.0 µm²	Yes	No
Image Surface area differ	0.239 %	Yes	No
Image Rq	2.87 nm	Yes	No
Image Ra	1.88 nm	Yes	No
Image Rmax	35.0 nm	Yes	No
Raw mean	-0.054...	Yes	No
Mean	-0.054...	Yes	No
Z Range	17.0 nm	Yes	No
Surface area	2.31 µm²	Yes	No
Projected surface area	2.31 µm²	Yes	No
Surface area difference	0.149 %	Yes	No
Rq	1.65 nm	Yes	No
Ra	1.13 nm	Yes	No
Rmax	17.1 nm	Yes	No
Skewness	2.29 nm	Yes	No
Kurtosis	14.2 nm	Yes	No
Rz	0.00 nm	Yes	No
Rz Count	0.00	Yes	No
Max peak ht (Rp)	0.00 nm	Yes	No
Av max ht (Rpm)	0.00 nm	Yes	No
Max depth (Rv)	0.00 nm	Yes	No
Av max depth (Rvm)	0.00 nm	Yes	No
Line density	0.00 /µm	Yes	No
Box x dimension	2.45 µm	Yes	No
Box y dimension	0.941 µm	Yes	No

Fig. S4. AFM images of the as-prepared Ni_3Fe films.

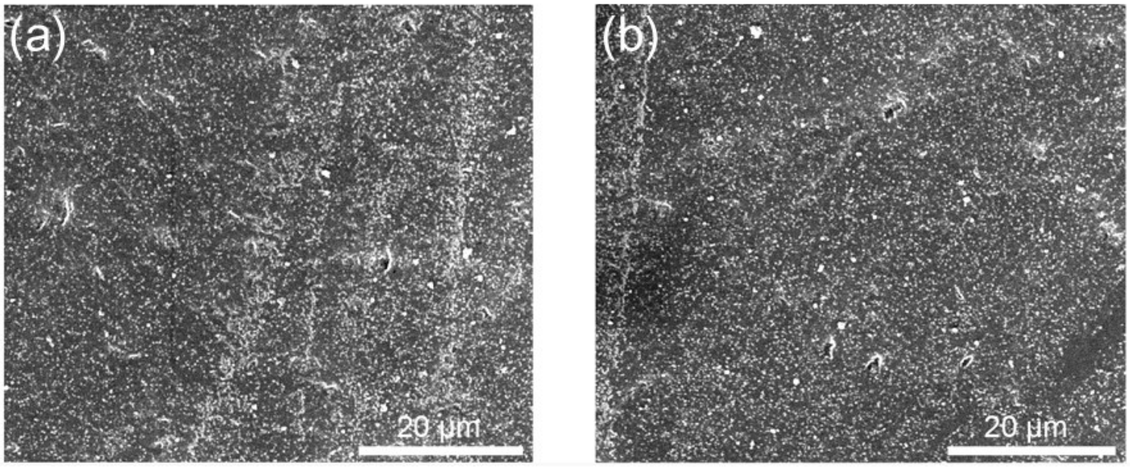

Fig. S5. SEM images of the as-prepared (a) and after straining test (b) Ni_3Fe films.

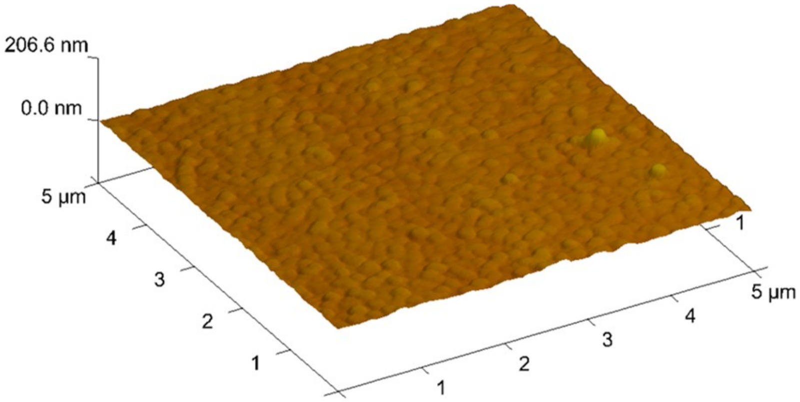

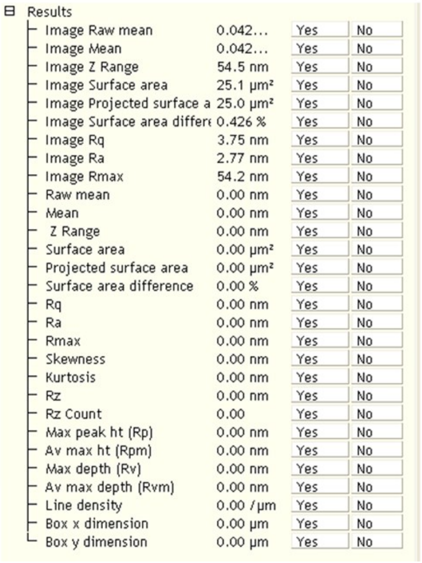
Results

Image Raw mean	0.042...	Yes	No
Image Mean	0.042...	Yes	No
Image Z Range	54.5 nm	Yes	No
Image Surface area	25.1 µm²	Yes	No
Image Projected surface a	25.0 µm²	Yes	No
Image Surface area differ	0.426 %	Yes	No
Image Rq	3.75 nm	Yes	No
Image Ra	2.77 nm	Yes	No
Image Rmax	54.2 nm	Yes	No
Raw mean	0.00 nm	Yes	No
Mean	0.00 nm	Yes	No
Z Range	0.00 nm	Yes	No
Surface area	0.00 µm²	Yes	No
Projected surface area	0.00 µm²	Yes	No
Surface area difference	0.00 %	Yes	No
Rq	0.00 nm	Yes	No
Ra	0.00 nm	Yes	No
Rmax	0.00 nm	Yes	No
Skewness	0.00 nm	Yes	No
Kurtosis	0.00 nm	Yes	No
Rz	0.00 nm	Yes	No
Rz Count	0.00	Yes	No
Max peak ht (Rp)	0.00 nm	Yes	No
Av max ht (Rpm)	0.00 nm	Yes	No
Max depth (Rv)	0.00 nm	Yes	No
Av max depth (Rvm)	0.00 nm	Yes	No
Line density	0.00 /µm	Yes	No
Box x dimension	0.00 µm	Yes	No
Box y dimension	0.00 µm	Yes	No

Fig. S6. AFM images of the Ni_3Fe films after the strain test.

References

1. S. Wannakao, T. Maihom, K. Kongpatpanich, J. Limtrakul and V. Promarak, *Phys. Chem. Chem. Phys.*, 2017**, 19(43)**, 29540-29548.

2. G. Kresse and J. Furthmüller, *Phys. Rev. B*, 1996, **54 (16)**, 11169-11186.

3. J. P. Perdew, K. Burke and M. Ernzerhof, *Phys. Rev. Lett.*, 1996, **77 (18)**, 3865-3868.

4. P. E. Blöchl, *Phys. Rev. B*, 1994, **50 (24)**, 17953-17979.

5. H. J. Monkhorst and J. D. Pack, *Phys. Rev. B*, 1976**,13 (12)**, 5188-5192.

6. K. Yan, T. Adit Maark, A Khorshidi, V. Sethuraman, A. Peterson, P. Guduru. *Angew. Chem. Int. Edit.* 2016, **55**, 6175-6181.